Au-ACRAMTU-PEt$_3$ Alters Redox Balance To Inhibit T Cell Proliferation and Function[#]

P. Kent Langston[*], **Mu Yang**[†], **Ulrich Bierbach**[†], **Derek Parsonage**[‡], **Leslie B. Poole**[‡], **Madeline J. Price**[*], and **Jason M. Grayson**[*]

[*]Department of Microbiology and Immunology Wake Forest University School of Medicine Winston-Salem, NC 27157, USA

[‡]Department of Biochemistry Wake Forest University School of Medicine Winston-Salem, NC 27157, USA

[†]Department of Chemistry Wake Forest University Winston-Salem, NC 27109, USA

Abstract

Although T cells play a critical role in protection from viruses, bacteria and tumors, they also cause autoimmune diseases such as systemic lupus erythematosus (SLE), rheumatoid arthritis (RA), and multiple sclerosis (MS). Unwanted T cell responses during organ transplant, graft versus host disease (GVHD), and allergies are also major clinical problems. While drugs are available to suppress unwanted immune responses they have limited efficacy with serious side effects. Thus new therapeutics limiting T cell activation, proliferation and function can make an immediate clinical impact. To identify new suppressors of lymphocyte activation, proliferation and function, we examined the immunosuppressive activity of gold(I) analogues of platinum-acridine antitumor agents. We found that the gold complex, Au-ACRAMTU-PEt$_3$ is a potent suppressor of murine and human T cell activation. Preincubation with Au-ACRAMTU-PEt$_3$ suppresses the proliferation of CD4$^+$ and CD8$^+$ T cells at a similar concentration as pharmaceutical grade cyclosporine A. Au-ACRAMTU-PEt$_3$ pretreatment decreases the production of IFNγ, TNFα, IL-2, and IL-17 by human and murine CD4$^+$ and CD8$^+$ T cells. When mice were treated with Au-ACRAMTU-PEt$_3$ during viral infection the expansion of virus-specific CD8$^+$ T cells was decreased 10-fold and viral load was elevated. Taken together these results demonstrate that Au-ACRAMTU-PEt$_3$ has potent immunosuppressive activity that could be used to suppress immune responses during transplantation and autoimmunity.

Introduction

T cells are critical for protection from viruses, bacteria and tumors (1). Prior to infection, naïve T cells exist in a quiescent, nondividing state (2) relying on oxidative phosphorylation to meet metabolic needs (3). However during infection, if a naïve T cell encounters a mature

[*]Address correspondence to: Jason M. Grayson, Ph.D., Wake Forest University School of Medicine, 575 Patterson Avenue, Wake Forest Biotech Place, Winston-Salem, NC 27101, Phone Number: 336-716-0268, Fax Number: 336-716-9928, jgrayson@wakehealth.edu.

dendritic cell presenting cognate antigen, costimulatory molecules and inflammatory cytokines it will become activated (4, 5). During this process a wave of tyrosine phosphorylation and calcium influx occurs that programs new gene expression and drives the cell to enter S phase (6). Following the first division at ~24-48 hours, T cells begin a program of sustained division that allows them to divide up to 10 to 12 times. In addition to elaborating biological functions through clonal expansion, T cells also produce a wide range of cytokines including IL-2, IL-4, IL-17, TNFα, and IFNγ (7). Cytotoxic T lymphocytes (CTL) also use perforin and granzyme-mediated mechanisms to lyse infected cells (1). Following pathogen clearance, effector T cells enter a contraction phase. From 8 to 35 days postinfection antigen-specific T cell numbers decrease 10-fold and the surviving cells differentiate into memory T cells. These cells will be maintained for the life of the animal and can rapidly respond to prevent or ameliorate disease upon reinfection.

While they can perform protective functions during infection and cancer, T cells also cause disease. As part of their normal development, both the B and T cell pools are purged of self-reactive cells through apoptosis (8) and receptor editing (9). Although these mechanisms are highly efficient, they are not perfect, and some self-reactive cells slip through the developmental checkpoints and emigrate to the periphery. Outside of the thymus and bone marrow, multiple mechanisms such as regulatory T cells (10), anergy, (11) and activation induced cell death (AICD) (12) exist to maintain peripheral tolerance. But for reasons not entirely well understood related to infection, diet and genetics, tolerance breaks down and autoreactive T cells expand and cause disease. Examples of this include autoimmune diseases, such as systemic lupus erythematosus (SLE) (13), rheumatoid arthritis (RA) (14), and multiple sclerosis (MS) (15) where immune response are inappropriately generated against self. In all three of these diseases, self-reactive B and T cells must expand from a low precursor frequency and elaborate effector functions including cytokine production for disease to occur. While self-reactive responses are an important problem, unwanted immune responses during organ transplant and graft-versus-host disease (GVHD) are also major clinical issues. Finally, many individuals suffer from allergies that are unwanted immune responses against innocuous environmental substances (16, 17). Taken together a large portion of clinical disease could be impacted if the activation, proliferation and function of lymphocytes could be precisely controlled.

Multiple drugs including cyclosporine, FK506 and rapamycin are available for immune suppression in transplantation and other settings, but they have unwanted side effects including hypertension and renal nephropathy that limit their efficacy (18-20). Therefore, because of this, other compounds including cancer drugs, such as methotrexate (21) and azathioprine (22), which target rapidly proliferating cells such as tumors or activated lymphocytes, have been used as immunosuppressives with some efficacy. To identify new suppressors of lymphocyte activation, proliferation and function, we examined the immunosuppressive activity of gold(I) thiourea complexes. Originally developed as treatments for tuberculosis, gold(I) thiourea complexes were found to have efficacy against rheumatoid arthritis. The compounds examined in this study include a series of cationic complexes in which gold is linearly coordinated by the thiourea sulfur of a 9-aminoacridine ligand or structurally related derivatives, and a *trans*-ligand including (pseudo) halides and phosphines (23). Although these gold based organometallic complexes had reduced

cytotoxicity against NCI-H460, a non-small-cell cancer cell line, they had anti-tuberculosis activity in the sub-micromolar range. We found that Au-ACRAMTU-PEt$_3$ (ACRAMTU = 1-[2-(acridin-9-ylamino)ethyl]-1,3-dimethylthiourea) is a potent suppressor of murine and human T cell activation. Preincubation with Au-ACRAMTU-PEt$_3$ suppresses the proliferation of CD4$^+$ and CD8$^+$ T cells at a similar concentration as commercially available cyclosporine A. Au-ACRAMTU-PEt$_3$ pretreatment decreases the production of IFNγ, TNFα, IL-2, and IL-17 by human and murine CD4$^+$ and CD8$^+$ T cells. When mice were treated with Au-ACRAMTU-PEt$_3$ during viral infection the expansion of virus-specific CD8$^+$ T cells was decreased 10-fold and viral load was increased. Taken together these results demonstrate that Au-ACRAMTU-PEt$_3$ has potent immunosuppressive activity and could be used to suppress immune responses during transplantation and autoimmunity.

Materials and Methods

Mice and viral infections

Six- to eight-week-old female C57BL/6 mice were purchased from the National Cancer Institute (Frederick, MD). Mice were infected with 2×10^5 pfu LCMV-Armstrong intraperitoneally and used at the indicated time points. Virus was grown and quantitated as previously described (24). All studies were approved by the Institutional Animal Care and Use Committee (IACUC) of the Wake Forest School of Medicine.

Cell isolation

Spleens were removed from mice following cervical dislocation. After teasing apart the spleen on a wire mesh screen, red blood cells were osmotically lysed using ACK Lysis Buffer (Lonza). Splenocytes were resuspended in complete media containing RPMI 1640 supplemented with 10% fetal calf serum (FCS, HyClone), L-glutamine (HyClone), penicillin-streptomycin (Cellgro), non-essential amino acids (GIBCO), and 2-mercaptoethanol (GIBCO). Thymocytes were prepared in a similar manner. To isolate bone marrow cells, both femurs were flushed with complete media. Red blood cells were osmotically lysed as described above, and then cells were washed and counted. Venous blood was drawn from healthy volunteers after approval from the Wake Forest University School of Medicine Institutional Review Board (IRB). Peripheral blood mononuclear cells (PBMCs) were isolated using LymphoPrep media according to the manufacturer's instructions.

Adoptive transfer and effector CD8$^+$ T cell generation

A naïve P14 Thy1^{a}PL/1 mouse was sacrificed and the spleen was excised. After osmotic lysis, splenocytes were stained with Abs specific for CD8α, CD90.1, and D^{b}GP33-41 MHC class I tetramer. Splenocytes containing 10^5 naïve P14 CD8$^+$ T cells were transferred into naïve C57BL/6 mice with an engraftment of 10^4 cells (25). Mice were then infected with 2×10^5 pfu of lymphocytic choriomeningitis virus (LCMV) strain Armstrong by i.p. injection and were sacrificed on day 8 for effector cell isolation.

Surface and Intracellular Staining

In this study, the following antibodies were used: rat anti-mouse CD8-PerCP, rat anti-mouse CD8-APC, rat anti-mouse CD4-PerCP, rat anti-mouse CD44-FITC and PE, rat anti-mouse CD90.1-Pacific Blue, rat anti-mouse CD90.1-FITC, rat anti-mouse CD90.1-PE-Cy-7, rat anti-mouse CD62L-APC-Cy7, rat anti-mouse IFNγ-FITC, rat anti-mouse TNFα-PE, rat anti-mouse IL-2-APC, mouse anti-human-IFNγ-FITC, mouse anti-human- TNFα PE-Cy-7, mouse anti-human-IL-17-APC, rat anti-human-IL-2-FITC, mouse anti-human-CD4-PE, mouse anti-human-CD8 APC H7, rabbit anti-phospho-ERK1/2 (Tyr202/Tyr204) and rabbit anti-ZAP70 (T183,Y185). The phospho- antibodies were purchased from Cell Signaling. All other antibodies were purchased from BD Pharmingen. Surface staining was performed by incubating cells in a 1:100 dilution of antibody in 2% FACS Buffer (phosphate buffered saline (PBS) plus 2% FCS) for 30 minutes on ice. Cells were washed three times with FACS Buffer and fixed in 2% paraformaldehyde (Sigma-Aldrich, St. Louis, MO). After three washes, intracellular cytokine staining was performed using the BD Cytofix/Cytoperm kit (with GolgiPlug and GolgiStop) according to the manufacturer's protocol. 7-amino actinomycin D (7-AAD) was added as a surface stain to identify viable cells.

For phospho-ERK1/2, and phospho-ZAP70 staining, purified CD8$^+$ T cells were fixed in 2% paraformaldehyde at 37°C for 10 min after stimulation. Samples were then permeabilized with 90% methanol prior to antibody staining according to Cell Signaling's protocol. Samples were acquired on a BD FACSCanto instrument and analyzed using FlowJo software (TreeStar, San Francisco, CA).

5-(and-6)-chloromethyl-2′,7′-dichlorodihydrofluorescein diacetate, acetyl ester oxidation (DCFDA) and Mitosox labeling

DCFDA was purchased from Invitrogen and resuspended in DMSO as a 2mM stock. Cells were incubated in a 96 well round bottom plate with drug and were loaded with 5μM DCFDA for 30 minutes at 37°C in complete media and acquired immediately on a FACSCanto instrument. Mitosox was brought up as 5 mM stock in DMSO and cells were loaded in 5μM dye for 30 minutes in the presence of drug at 37°C.

Data are presented as change in mean fluorescent intensities compared to vehicle-treated cells.

T cell purification

Naïve CD4$^+$ or CD8$^+$ T cells were negatively selected by magnetic bead enrichment from the spleens of naïve C57BL/6 mice using the Miltenyi MicroBead system according to the manufacturer's protocol. For human T cell isolation either the naïve CD4$^+$ or CD8$^+$ T cell isolation kit was used. Purity was >95% as determined by flow cytometry.

CTL line generation

Naïve CD8$^+$ T cells were negatively selected by magnetic bead enrichment from the spleens of naïve C57BL/6 mice using the Miltenyi MicroBead system according to the manufacturer's protocol. 5×10^5 purified CD8$^+$ T cells were cultured in media containing 2U/ml recombinant murine IL-12 (5) with 10μg/ml antiCD3/CD28 stimulation for 2 days.

On day 2 cells were removed from antibody coated wells and allowed to rest overnight before drug treatment and restimulation.

Synthesis of Gold(I) Complexes

The platinum (26) and gold compounds (23) were synthesized according to published procedures, except for Au-ACRAMTU-PEt$_3$, for which an improved method was developed: To a suspension of 0.097 g (0.25 mmol) of 1-[2-(acridin-9-ylamino)ethyl]-1,3-dimethylthiourea (ACRAMTU, nitrate salt) in mixture of 15 mL of methanol and 3 mL water was added 0.092 g (0.263 mmol) of chlorotriethylphosphinegold(I). After brief stirring the suspension turned into a clear solution, and 0.042 g (0.25 mmol) of AgNO$_3$ in a minimum amount of water was added. Precipitated AgCl was removed by syringe filtration and the solvent was removed by rotary evaporation. The resulting oily material was dried in an oil pump vacuum for 2 h to remove residual water. Dichloromethane (10 mL) was added, and the mixture was stored in the refrigerator for 2 h. Au-ACRAMTU-PEt$_3$ (systematic formula: [Au(ACRAMTU)PEt$_3$](NO$_3$)$_2$) crystallized as a yellow microcrystalline solid, which was recovered by filtration and under vacuum. Yield: 0.135 g (77%).

CFSE labeling

CFSE (5-6-carboxyfluorescein diacetate, succinimidyl ester, Molecular Probes) was resuspended in DMSO as a 5 mM stock and stored at −20°C. Magnetically-purified T cells were washed three times in cold PBS and resuspended at a concentration of 2×10^6 cells/ml in PBS. The CFSE stock was diluted to 6.67 μM in PBS and mixed 1:1 (v/v) with cells, resulting in a final concentration of 3.33 μM CFSE. After 3 min, samples were vortexed and then incubated for an additional 2 min. One tenth volume of FCS was added, and the cells were vortexed and then incubated for an additional 60 s. The cells were washed three times with complete media and used in experiments.

Proliferation parameter analysis

The division and proliferative indices and the percent divided parameters were calculated using the Proliferation Platform in the FloJo software package.

Calcium flux assay

Fura-Red-acetoxymethyl ester (AM) and Fluo-3-AM were purchased from Molecular Probes and dissolved in DMSO as 1 mM and 1.25 mM stocks, respectively. Magnetically-purified CD8$^+$ T cells were incubated with 5 μM Fura-Red AM and 2.5 μM Fluo-3-AM in PBS containing 5% FCS for 30 min at 37°C in the presence of DMF control, or Au-ACRAMTU-PEt$_3$. Samples were washed two times with PBS supplemented with 5% FCS and resuspended in the same media containing DMF control, or Au-ACRAMTU-PEt$_3$. Cells were coated with biotin-labeled anti-CD3 and anti-CD8α, acquired for 60 s on the FACSCalibur Flow Cytometer, after which 5μg/ml streptavidin was added to the sample and recording was resumed.

Cell proliferation assay

Drugs were dissolved in N,N-dimethylformamide (DMF) as 2 mg/ml stocks. Each drug was then diluted in pre-warmed complete medium to make a 20 μg/ml solution. In the right-most column of a 96-well flat-bottom plate, each 20 μg/ml drug was again diluted 1:3 in the same medium and subsequently diluted across its respective row (from right-to-left) in a series of 2-fold dilutions. Isotype, vehicle, and rotenone controls were included in the bottom row of each plate. Isotype and vehicle wells received a 0.3% DMF solution, while rotenone wells received a 10 μM solution of rotenone in pre-warmed complete medium. Magnetically-purified $CD4^+$ or $CD8^+$ T cells from the spleens of naïve C57BL/6 mice were then added to the plate and incubated for 60 min at 37°C. After incubation, the cells were stimulated with plate-bound anti-CD3 (αCD3) and anti-CD28 (αCD28) antibodies (Abs) and returned to the incubator for 72 h. On day 3 post-stimulation, Celltiter 96 Aqueous One Solution from Promega was added to each well according to the manufacturer's protocol. Absorbance was read at 490 nm with a 96-well plate reader every 10 min for 2 h. To calculate the increase in metabolic activity over isotype vehicle-treated cells, the difference between each absorbance and the average isotype absorbance was divided by the difference between the average vehicle and average isotype absorbance. The quotient was then multiplied by 100% to obtain the percent specific increase for each well.

In vitro stimulation

For CD3/CD28-stimulation, 96-well flat-bottom plates were coated with 10 μg/ml anti-CD3 (αCD3) and anti-CD28 (αCD28) overnight at 4°C. For CD3/CD8 stimulation, purified T cells were coated for 1 minute with 5μg/ml biotin-labeled CD3 and 1μg/ml biotin-labeled anti-CD8α. At the appropriate timepoint, activation was induced as described by Jia et al (27) by cross-linking with 5μg/ml streptavidin.

Au-ACRAMTU-PEt$_3$ treatment

Solid Au-ACRAMTU-PEt$_3$ was dissolved in sterile PBS and given intraperitoneally at 6 mg/kg. Four hours later, mice were infected with LCMV-Armstrong. A maintenance dose was administered to the mice every 12 hours for the duration of treatment.

Statistical Analysis

Data from vehicle and Au-ACRAMTU-PEt$_3$-treated mice were analyzed using a two-tailed Student's *t*-test. A p-value of   0.05 was considered significant.

Results

Proliferation of naïve murine and human CD8$^+$ and CD4$^+$ T cells is inhibited by Au-ACRAMTU-PEt$_3$

To determine whether anticancer transition metal complexes have an inhibitory effect on the activation and proliferation of naïve $CD8^+$ T cells, a high-throughput colorimetric cell proliferation assay utilizing a tetrazolium compound [3-(4,5-dimethylthiazol-2-yl)-5-(3-carboxymethoxyphenyl)-2-(4-sulfophenyl)-2H-tetrazolium, inner salt; MTS] was performed. In metabolically active cells, MTS becomes reduced to a soluble formazan product that

absorbs at 490 nm. At inhibitory concentrations of drug, wells containing murine naïve $CD8^+$ T cells that have been stimulated with plate-bound anti-CD3 (αCD3) and anti-CD28 (αCD28) Abs appear yellow and absorb minimally at 490 nm. Wells containing non-inhibitory concentrations of drug have higher total metabolic activity associated with cell growth and proliferation, turning the media a dark brown color and absorbing strongly at 490 nm. Fig. 1A demonstrates the concentration-dependent effect of several anticancer drugs on T cell proliferation. Pharmaceutical-grade cyclosporine A (CsA) was included as a control. Three gold-based and one platinum-based agent along with the carrier ligand ACRAMTU were tested. Of the compounds screened, only the phosphine-substituted cationic complex, Au-ACRAMTU-PEt$_3$, had a significant effect on proliferation at submicromolar concentrations. The percent specific increase in absorbance over isotype was calculated across the range of concentrations used for each drug, and sigmoidal dose-response curves were generated. Fig. 1B demonstrates the efficacy of Au-ACRAMTU-PEt$_3$ as an inhibitor of naïve $CD8^+$ T cell activation and proliferation. Importantly, the inhibition is comparable to that of pharmaceutical-grade CsA and this effect is not seen with the ACRAMTU ligand alone. Indeed, the half maximal inhibitory concentrations (IC$_{50}$) of CsA and Au-ACRAMTU-PEt$_3$, derived from their dose-response curves, are nearly identical (Fig. 1C). The efficacy of Au-ACRAMTU-PEt$_3$ as an inhibitor of $CD4^+$ T cell activation and proliferation was also found to be comparable to that of CsA (Fig. 1D) with similar IC$_{50}$'s (Fig. 1E).

Since the MTS assay is influenced by cell growth, death, and metabolic status, the ability of Au-ACRAMTU-PEt$_3$ to inhibit T cell proliferation was determined by assessing CFSE (5-6-carboxyfluorescein diacetate, succinimidyl ester) dilution. $CD8^+$ T cells and $CD4^+$ T cells were magnetically purified from the spleens of naïve C57BL/6 mice by negative selection and then labeled with CFSE. Purified, labeled $CD8^+$ and $CD4^+$ T cells were treated with vehicle or drug across a range of concentrations for 60 min, after which cells were transferred to a plate coated with αCD3/αCD28 or isotype Abs and incubated for 3 days. In this assay, Au-ACRAMTU-PEt$_3$ inhibited proliferation at low nanomolar concentrations (Fig. 1F). Consistent with the MTS results, proliferation of $CD4^+$ T cells was inhibited at lower concentrations of Au-ACRAMTU-PEt$_3$ than what was required to inhibit $CD8^+$ T cell proliferation. Thus, proliferation of naïve murine $CD8^+$ and $CD4^+$ T cells following stimulation with αCD3 and αCD28 Abs is inhibited by preincubation with Au-ACRAMTU-PEt$_3$.

To measure the ability of Au-ACRAMTU-PEt$_3$ to inhibit human T cell proliferation, $CD8^+$ T cells and $CD4^+$ T cells were magnetically purified from the blood of healthy human donors by positive selection and then labeled with CFSE. Purified, labeled $CD8^+$ and $CD4^+$ T cells were treated with vehicle or drug across a range of concentrations for 60 min, after which cells were transferred to a plate coated with αCD3/αCD28 or isotype Abs and incubated for 5 days. Similar to the effect on murine T cells, Au-ACRAMTU-PEt$_3$ inhibited proliferation of human $CD8^+$ and $CD4^+$ T cells (Fig. 1F). Quantitation of the effects of Au-ACRAMTU-PEt$_3$ on T cell proliferation and viability is presented in Supplemental Figure 1.

Au-ACRAMTU-PEt$_3$ incubation inhibits calcium flux and phosphorylation of ERK1/2 in CD8$^+$ T cells

Phosphorylation of ZAP70 is a key early step in T cell activation that increases the kinase activity of the protein. Intracellular staining revealed that there was a ~1.2-fold increase in the mean fluorescent intensity (m.f.i.) of ZAP70 phosphorylation within 2 minutes of CD3 and CD8 stimulation (Fig. 2A). Treatment of cells with 274 nM Au-ACRAMTU-PEt$_3$ did not decrease phosphorylation. H$_2$O$_2$ was used as a positive control for ZAP70 phosphorylation because it decreases total phosphatase activity. Flux of Ca^{2+} through the CRAC (calcium release-activated calcium) channel is another early process that is critical for T cell activation. To determine whether Au-ACRAMTU-PEt$_3$ prevents T cell proliferation by interfering with Ca^{2+} flux, magnetically purified naïve CD8$^+$ T cells were incubated with both Au-ACRAMTU-PEt$_3$ and the Ca^{2+}-specific dyes Fura-Red-acetoxymethyl ester (AM) and Fluo-3-AM. Cells incubated with a 0.3% DMF (N,N-dimethylformamide) control had a basal level of Ca^{2+}, which rapidly increased following incubation with biotin-labeled anti-CD3 and antiCD8α followed by streptavidin crosslinking; however, cells treated with Au-ACRAMTU-PEt$_3$ exhibited decreased Ca^{2+} flux following stimulation (Fig. 2B). We next examined the effect of Au-ACRAMTU-PEt$_3$ incubation on MAP kinase signaling. Incubation with biotin-labeled isotype antibodies elicited phospho-ERK1/2 staining that was indistinguishable from its isotype control (Fig. 2C). After 5 minutes of CD3/CD8 stimulation the m.f.i. of phospho-ERK1/2 staining increased ~1.6-fold in vehicle-treated cells but in cells treated with Au-ACRAMTU-PEt$_3$ there was no change in staining.

Incubation with Au-ACRAMTU-PEt$_3$ disrupts the mitochondrial thioredoxinthioredoxin reductase system and oxidizes CD8$^+$ T cells

Previous studies have identified mitochondrial thioredoxin reductase II (TrxR2) as a potential target of Et$_3$PAu(I) complexes (28). To determine the effect of Au-ACRAMTU-PEt$_3$ on the function of TrxR2, naïve splenocytes and magnetically purified CD8$^+$ T cells were treated with either vehicle, 4.36 μM Au-ACRAMTU-PEt$_3$, 10 mM H$_2$O$_2$, or 20 mM dithiothreitol (DTT). Following precipitation of proteins and incubation of sonicated cells in 15 mM 4-acetoamido-4′-maleimidylstilbene-2,2′-disulfonic acid (AMS) for 3 h, proteins were separated on a 15% polyacrylamide separating gel, transferred to a nitrocellulose membrane, and probed for thioredoxin II (Trx2) using a polyclonal IgG anti-Trx2 Ab. Splenocytes treated with vehicle had approximately a 1:1 ratio of reduced to oxidized Trx2; however, Au-ACRAMTU-PEt$_3$-treated splenocytes had primarily the oxidized form of Trx2 (Supplemental Figure 2A). The difference in the oxidation state of Trx2 in vehicle- and Au-ACRAMTU-PEt$_3$-treated CD8$^+$ T cells was even more pronounced. This finding demonstrates that incubation with Au-ACRAMTU-PEt$_3$ interferes with the Trx2-TrxR2 redox system, causing a shift from reduced to oxidized Trx2 in naïve CD8$^+$ T cells.

Because we observed changes in the oxidation of mitochondrial thioredoxin, we measured whether steady state levels of reactive oxygen intermediates (ROI) were altered following Au-ACRAMTU-PEt$_3$ incubation. Short-term (30 minutes) incubation with 274 nM Au-ACRAMTU-PEt$_3$ modestly, but reproducibly, increased the m.f.i. (Fig. 2D) of DCFDA, which measures cellular peroxides, and MitoSox which allows the levels mitochondrial

superoxide to be determined. Representative primary data are presented in Supplemental Figure 2B and C. To determine whether the shift in intracellular redox balance blocks activation, naïve $CD8^+$ T cells were magnetically purified from the spleens of C57BL/6 mice by negative selection and CFSE labeled. $CD8^+$ T cells were pretreated for 1 h with either media or 5 mM N-acetyl cysteine (NAC) followed by treatment with media or 274 nM Au-ACRAMTU-PEt_3 for 1 h. Following incubation with drug, $CD8^+$ T cells were transferred to a plate coated with αCD3/αCD28 or isotype Abs and incubated for 3 days. Pretreatment with 5 mM NAC modestly inhibited proliferation (Supplemental Figure 2D-H); however, as in our prior results incubation with 274 nM Au-ACRAMTU-PEt_3 prevented proliferation (Fig. 2E). When naïve $CD8^+$ T cells were pretreated with 5 mM NAC and subsequently incubated with 274 nM Au-ACRAMTU-PEt_3, activation and proliferation were restored to the level observed with NAC alone (Fig. 2E and Supplemental Figure 2). To determine the molecular mechanism by which NAC rescues the proliferative block of Au-ACRAMTU-PEt_3 we repeated our signal transduction analysis. Incubation of T cells with NAC and Au-ACRAMTU-PEt_3 failed to rescue the block in Ca^{2+} flux (data not shown), but preincubation with 5mM NAC followed by Au-ACRAMTU-PEt_3 treatment resulted in a restoration of ERK1/2 phosphorylation (Fig. 2F). Signal transduction data from multiple experiments are quantitated in Supplemental Figure 3. Thus Au-ACRAMTU-PEt_3 inhibits T cell activation and proliferation by modulating cellular redox status that controls ERK1/2 phosphorylation.

Au-ACRAMTU-PEt_3 incubation decreases $CD8^+$ T cell cytokine production and degranulation

Since Au-ACRAMTU-PEt_3 incubation decreased Ca^{2+} flux, ERK1/2 phosphorylation and activation, we next sought to determine if Au-ACRAMTU-PEt_3 could impact $CD8^+$ T cell function. Splenocytes containing 10^5 naïve P14 $CD90.1^+$ TCR transgenic $CD8^+$ T cells were transferred into naïve C57BL/6 mice, which were subsequently infected with 2×10^5 pfu of lymphocytic choriomeningitis virus (LCMV)-Armstrong. To measure effector T cell function, mice were sacrificed on day 8 postinfection (p.i.) and intracellular cytokine staining was performed for IFNγ, TNFα, and IL-2 following pretreatment with vehicle or Au-ACRAMTU-PEt_3 and stimulation with GP33-41 peptide *in vitro*. Incubation with Au-ACRAMTU-PEt_3 significantly reduced the percent of LCMV-specific $CD8^+$ $CD90.1^+$ T cells capable of producing cytokines following GP33-41 stimulation (Fig. 3A and B). The inhibition achieved with Au-ACRAMTU-PEt_3 incubation was concentration dependent (Fig. 3B). To determine whether Au-ACRAMTU-PEt_3 is capable of inhibiting human $CD8^+$ T cell function, the production of IFNγ, TNFα, and IL-2 was assessed following pretreatment with vehicle or Au-ACRAMTU-PEt_3 and stimulation with PMA/ION *in vitro*. Incubation with Au-ACRAMTU-PEt_3 significantly reduced the percent of human $CD8^+$ T cells that produced cytokines following PMA/ION stimulation compared to vehicle-treated cells (Fig. 3C and 3D). The inhibition achieved with Au-ACRAMTU-PEt_3 was dependent upon the concentration used, with 4.36 μM resulting in the greatest decrease (Fig. 3D). Importantly short-term incubation with micromolar concentrations of Au-ACRAMTU-PEt_3 did not decrease the viability of total PBMCs, $CD8^+$ or $CD4^+$ T cells (Supplemental Figure 4).

To determine the effect of Au-ACRAMTU-PEt_3 on cytolytic activity, a similar adoptive transfer and infection approach were used, and splenocytes from mice sacrificed on day 8

p.i. were pretreated with vehicle or Au-ACRAMTU-PEt$_3$ followed by incubation with anti-CD107a and anti-CD107b Abs during *in vitro* stimulation with GP33-41 peptide. Since CD107a and b are expressed on the cell surface when T cells degranulate, their expression can be used as a surrogate for cytolysis. Following GP33-41 stimulation, the percent of CD8$^+$ CD90.1$^+$ T cells expressing CD107a and b was determined. As expected, the percent of LCMV-specific CD8$^+$ CD90.1$^+$ T cells that degranulated following stimulation with GP33-41 peptide was significantly reduced by preincubation with Au-ACRAMTU-PEt$_3$ compared to vehicle (Fig. 3E and F). Thus, Au-ACRAMTU-PEt$_3$ incubation significantly decreases LCMV-specific effector CD8$^+$ T cell degranulation *in vitro*.

Au-ACRAMTU-PEt$_3$ incubation decreases murine and human CD4$^+$ T cell cytokine production *in vitro*

Given the effect of Au-ACRAMTU-PEt$_3$ on effector CD8$^+$ T cell function, we next sought to determine if Au-ACRAMTU-PEt$_3$ incubation could also modulate CD4$^+$ T cell cytokine production. Naïve C57BL/6 mice were infected with 2×10^5 pfu of LCMV-Armstrong. To measure T cell function, mice were sacrificed on day 8 p.i. and intracellular cytokine staining was performed for IFNγ, TNFα, and IL-2 following pretreatment with vehicle or Au-ACRAMTU-PEt$_3$ and stimulation with GP61-80 peptide *in vitro*. The percent of CD4$^+$ T cells that produced cytokines following GP61-80 stimulation was significantly reduced by Au-ACRAMTU-PEt$_3$ in a concentration dependent manner (Fig. 4A-C). To determine whether Au-ACRAMTU-PEt$_3$ is also capable of inhibiting human CD4$^+$ T cell function, intracellular cytokine staining was performed for IFN-γ, TNF-α, IL-2, IL-17, and IL-4 following pretreatment with vehicle or Au-ACRAMTU-PEt$_3$ and stimulation with PMA/ION *in vitro*. Incubation with Au-ACRAMTU-PEt$_3$ significantly reduced the percent of human CD4$^+$ T cells that produced IFN-γ, TNF-α, IL-2, and IL-17 following PMA/ION stimulation (Fig. 4D-F) but increased the percent of CD4$^+$ T cells that produced IL-4 (Fig. 4H) compared to vehicle-treated cells. Modulation of CD4$^+$ T cell cytokine production resulting from incubation with Au-ACRAMTU-PEt$_3$ was concentration dependent (Fig. 4G and 4I). Thus, Au-ACRAMTU-PEt$_3$ incubation significantly decreases production of IFN-γ, TNF-α, IL-2, IL-17 by CD4$^+$ T cells while increasing production of IL-4.

Au-ACRAMTU-PEt$_3$ incubation decreases CD8$^+$ T cell cytokine production *in vitro* in an autonomous manner

Our functional assays using heterogenous mixtures of cells such as splenocytes or PBMCs required a higher concentration of Au-ACRAMTU-PEt$_3$ to achieve inhibition than those using purified naïve T cells. To determine if effector T cells could be inhibited at lower concentrations we first purified murine CD8$^+$ T cells and then activated them with anti-CD3 and anti-CD28 in the presence of IL-12 as described previously (4, 5). After 2 days, cells were removed from CD3/CD28 stimulation and allowed to rest 24 hours followed by pretreatment with increasing Au-ACRAMTU-PEt$_3$, and cytokine production was measured following PMA and ION stimulation. When the production of IFN-γ and TNF-α was examined (Fig. 5 A, B and C) there was a significant decrease in both the percentage of cells that produced either cytokine and their m.f.i. Similar results were observed for IL-2 (Fig. 5D). Interestingly, when purified T cells were used significant defects in cytokine production

could be observed at 274 nM Au-ACRAMTU-PEt$_3$. Thus low nanomolar Au-ACRAMTU-PEt$_3$ inhibits cytokine production in a T cell autonomous manner.

The expansion of CD8$^+$ T cells is reduced in Au-ACRAMTU-PEt$_3$-treated mice following acute infection

Due to the profound effect of Au-ACRAMTU-PEt$_3$ incubation on T cell activation, proliferation, and function *in vitro*, we hypothesized that treating C57BL/6 mice with this drug during the expansion phase following an acute viral infection would significantly decrease the T cell response. Naïve C57BL/6 mice were treated with 6 mg/kg of Au-ACRAMTU-PEt$_3$ every 12 hours for 8 days, at which point the mice were sacrificed and the spleen, lymph nodes, bone marrow, and thymus were removed. Administering Au-ACRAMTU-PEt$_3$ resulted in a 10-fold reduction in the total number of CD8$^+$CD4$^+$ DP T cells in the thymus while the total number of CD8$^+$ and CD4$^+$ SP T cells in the thymus, spleen, lymph nodes, and bone marrow (Fig. 6A-C) were minimally affected. To test the hypothesis that Au-ACRAMTU-PEt$_3$ treatment would decrease CD8$^+$ T cell expansion following acute viral infection, splenocytes containing 10^5 naïve P14 CD8$^+$ T cells were transferred into naïve C57BL/6 mice, which were subsequently infected with LCMV-Armstrong. From days 0 to 8 p.i., mice were injected i.p. with 6 mg/kg of Au-ACRAMTU-PEt$_3$ every 12 h. Mice were sacrificed at the peak of the antiviral T cell response on day 8 p.i., and the number of CD8$^+$ CD90.1$^+$ effector T cells was determined. Treatment with Au-ACRAMTU-PEt$_3$ decreased the percentage (Fig. 6D) and number of CD8$^+$ CD90.1$^+$ T cells compared to vehicle-treated mice (Fig. 6E). Importantly, reduced antigen-specific T cells resulted in an increase in the viral titer in Au-ACRAMTU-PEt$_3$-treated mice (Fig. 6F). Taken together, these data demonstrate that Au-ACRAMTU-PEt$_3$ treatment can decrease the expansion of activated T cells *in vivo*.

Discussion

In this study, we have examined the effect of Au-ACRAMTU-PEt$_3$ treatment on T cell activation, proliferation, and function. Here, we report five novel observations. First, preincubation of murine and human T cells with Au-ACRAMTU-PEt$_3$ prevented activation and proliferation following stimulation with CD3 and CD28 Abs. Second, Au-ACRAMTU-PEt$_3$ incubation resulted in decreased calcium flux and ERK1/2 phosphorylation in CD8$^+$ T cells. Third, Au-ACRAMTU-PEt$_3$ incubation shifts the redox balance in cells to a more oxidized state and its anti-proliferative effects can be rescued by antioxidant treatment. Fourth, Au-ACRAMTU-PEt$_3$ incubation significantly decreased CD4$^+$ and CD8$^+$ T cell cytokine production *in vitro* in a concentration-dependent manner. Fifth, the expansion of rapidly proliferating effector CD8$^+$ T cells following an acute viral infection was significantly suppressed by twice daily treatment with Au-ACRAMTU-PEt$_3$. Taken together, these results demonstrate the efficacy of Au-ACRAMTU-PEt$_3$ as an inhibitor of T lymphocyte activation, proliferation, and function.

What are the mechanisms by which Au-ACRAMTU-PEt$_3$ inhibits T cell activation and proliferation? Based on our in vitro studies, T cell activation is inhibited at two early steps: calcium flux and ERK1/2 phosphorylation. Additionally, we demonstrate that Au-

ACRAMTU-PEt$_3$ pretreatment increases the steady state level of reactive oxygen species (ROS) in the mitochondria. In addition to playing a critical role in energy production, mitochondria are a major source of ROS during T cell activation (29). Following anti-CD3 or peptide stimulation, ROS including superoxide and hydrogen peroxide, are produced by both CD4$^+$ and CD8$^+$ T cells (30, 31). This production is essential as blocking it with antioxidants decreases the expansion of T and B cells in vitro and in vivo (32, 33). Following ROS production in T and B cells cysteine becomes reversibly oxidized to sulfenic acid (31, 34). Combined with our observations that Au-ACRAMTU-PEt$_3$ induces a shift from reduced to oxidized thioredoxin, these results are consistent with a model where drug addition induces mitochondrial oxidative stress resulting in altered signal transduction. Further support for this idea is provided by the observation that addition of NAC, an antioxidant, is able to protect against the antiproliferative effects of Au-ACRAMTU-PEt$_3$ by restoring ERK1/2 phosphorylation. Importantly two recent studies have demonstrated that ERK2 can undergo sulfenic acid modification (35, 36) that could inhibit its activation. Although ERK1 is dispensable for peripheral T cell activation and proliferation, ERK2 function is required to increase Bcl-xL mRNA levels while suppressing those of Bim (37). Loss of ERK2 function leads to decreased T cell survival that can be rescued by loss of Bim. In addition to direct oxidative modification of ERK1/2, it is possible that upstream regulators could become oxidized in Au-ACRAMTU-PEt$_3$ treated cells. Gorelik and colleagues demonstrated that oxidative modification of protein kinase Cδ contributed to ERK inactivation observed in Lupus T cells (38). A similar mechanism could be contributing to the effects of Au-ACRAMTU-PEt$_3$. Importantly the anti-proliferative effects of Au-ACRAMTU-PEt$_3$ were not restricted to in vitro experiments, as they were also observed in rapidly dividing double negative T cells in the thymus and effector CD8$^+$ T cells in the spleen during viral infection. Taken together these findings demonstrate that Au-ACRAMTU-PEt$_3$ increases oxidative stress to decrease lymphocyte proliferation in vitro and in vivo.

In addition to decreasing proliferation Au-ACRAMTU-PEt$_3$ also inhibits T cell cytokine production and degranulation. By what mechanism does Au-ACRAMTU-PEt$_3$ modulate T cell function? Using intracellular cytokine staining, we found that effector T cells exhibited a major decrease in cytokine production at nanomolar concentrations of Au-ACRAMTU-PEt$_3$. Again similar to proliferation we hypothesize that Au-ACRAMTU-PEt$_3$ alters redox homeostasis, inhibiting cytokine production. Interestingly, IL-2 production was more sensitive to Au-ACRAMTU-PEt$_3$ incubation than IFNγ or TNFα. This result is consistent with our observations of decreased calcium flux, as transcription of the IL-2 gene requires activation of the calcineurin-NFAT pathway following TCR stimulation (39). In addition to inhibiting cytokine production, Au-ACRAMTU-PEt$_3$ treatment also inhibited cytolytic activity of effector CD8$^+$ T cells. In contrast to the complete shutoff in cytokine production, Au-ACRAMTU-PEt$_3$ inhibited degranulation by 50%. Further support for the altered redox balance hypothesis is provided by increased production of IL-4 by CD4$^+$ T cells following Au-ACRAMTU-PEt$_3$ preincubation. Since dead cells are excluded from the analysis, this argues against toxicity decreasing all cytokine production, and instead supports our model of redox regulation, as prior reports have demonstrated that oxidizers such as mercuric chloride are able to induce IL-4 transcription in mast cells (40). Interestingly, PBMCs and

splenocytes required a higher concentration of Au-ACRAMTU-PEt$_3$ to inhibit cytokine production than purified effector CD8$^+$ T cells. One potential explanation could be that heterogenous mixtures such as PBMCs and splenocytes contain other cells that modulate the redox environment. Prior studies have shown that dendritic cells and monocytes modulate the extracellular redox environment to affect T cell proliferation and function (41). It is possible that the presence of these cells and their secretion of thioredoxin could alter the redox balance in T cells requiring more Au-ACRAMTU-PEt$_3$ to inhibit signaling.

In conclusion, our studies demonstrate that the gold(I) complex Au-ACRAMTU-PEt$_3$ is a potent inhibitor of T cell activation, proliferation, and function *in vitro* and *in vivo*. We have also advanced the current understanding of the mode of action of gold thiourea complexes by demonstrating that, in addition to interfering with the Trx2-TrxR2 redox system, Au-ACRAMTU-PEt$_3$ inhibits Ca^{2+}flux and ERK1/2 phosphorylation. Furthermore, we observed that twice-daily i.p. injections of 6 mg/kg of Au-ACRAMTU-PEt$_3$ were sufficient to decrease the effector CD8$^+$ T cell response to an acute viral infection 10-fold – a level of inhibition equivalent to that achieved with daily i.p. injections of 60 mg/kg of pharmaceutical-grade CsA (data not shown). Taken together, our observations *in vitro* and *in vivo* suggest that Au-ACRAMTU-PEt$_3$ may be used as a potential treatment for autoimmune diseases such as systemic lupus erythematosus and multiple sclerosis and for preventing rejection of transplanted tissues. Furthermore they highlight the key role that redox balance plays in the activation, proliferation and function of T cells. Finally, the mechanism of action of these mixed-ligand phosphine/thiourea complexes at the molecular level remains to be established. While the TrxR targeted [AuPEt$_3$] moiety appears to be a prerequisite for potent activity in vitro and in vivo, the role of the acridinylthiourea as a carrier ligand and its fate in circulation remain elusive. Thus, one goal of this drug development program will be to establish structure–activity relationships in libraries of structurally diverse derivatives.

Supplementary Material

Refer to Web version on PubMed Central for supplementary material.

References

1. Cui W, Kaech SM. Generation of effector CD8+ T cells and their conversion to memory T cells. Immunol Rev. 2010; 236:151–166. [PubMed: 20636815]

2. Di Rosa F, Ramaswamy S, Ridge JP, Matzinger P. On the lifespan of virgin T lymphocytes. J Immunol. 1999; 163:1253–1257. [PubMed: 10415021]

3. Chang CH, Curtis JD, Maggi LB Jr. Faubert B, Villarino AV, O'Sullivan D, Huang SC, van der Windt GJ, Blagih J, Qiu J, Weber JD, Pearce EJ, Jones RG, Pearce EL. Posttranscriptional control of T cell effector function by aerobic glycolysis. Cell. 2013; 153:1239–1251. [PubMed: 23746840]

4. Curtsinger JM, Johnson CM, Mescher MF. CD8 T cell clonal expansion and development of effector function require prolonged exposure to antigen, costimulation, and signal 3 cytokine. J Immunol. 2003; 171:5165–5171. [PubMed: 14607916]

5. Curtsinger JM, Lins DC, Mescher MF. Signal 3 determines tolerance versus full activation of naive CD8 T cells: dissociating proliferation and development of effector function. J Exp Med. 2003; 197:1141–1151. [PubMed: 12732656]

6. Fracchia KM, Pai CY, Walsh CM. Modulation of T Cell Metabolism and Function through Calcium Signaling. Front Immunol. 2013; 4:324. [PubMed: 24133495]

7. Zhu J, Yamane H, Paul WE. Differentiation of effector CD4 T cell populations (*). Annu Rev Immunol. 2010; 28:445–489. [PubMed: 20192806]

8. von Boehmer H, Kisielow P. Self-nonself discrimination by T cells. Science. 1990; 248:1369–1373. [PubMed: 1972594]

9. Tiegs SL, Russell DM, Nemazee D. Receptor editing in self-reactive bone marrow B cells. J Exp Med. 1993; 177:1009–1020. [PubMed: 8459201]

10. Schmidt A, Oberle N, Krammer PH. Molecular mechanisms of treg-mediated T cell suppression. Front Immunol. 2012; 3:51. [PubMed: 22566933]

11. Valdor R, Macian F. Induction and stability of the anergic phenotype in T cells. Semin Immunol. 2013; 25:313–320. [PubMed: 24211041]

12. Krammer PH, Arnold R, Lavrik IN. Life and death in peripheral T cells. Nat Rev Immunol. 2007; 7:532–542. [PubMed: 17589543]

13. Gualtierotti R, Biggioggero M, Penatti AE, Meroni PL. Updating on the pathogenesis of systemic lupus erythematosus. Autoimmun Rev. 2010; 10:3–7. [PubMed: 20863908]

14. Cooles FA, Isaacs JD. Pathophysiology of rheumatoid arthritis. Curr Opin Rheumatol. 2011; 23:233–240. [PubMed: 21427580]

15. Goverman JM. Immune tolerance in multiple sclerosis. Immunol Rev. 2011; 241:228–240. [PubMed: 21488900]

16. Jutel M, Akdis CA. Immunological mechanisms of allergen-specific immunotherapy. Allergy. 2011; 66:725–732. [PubMed: 21466562]

17. Jutel M, Akdis CA. T-cell subset regulation in atopy. Curr Allergy Asthma Rep. 2011; 11:139–145. [PubMed: 21271314]

18. Chapman JR, Nankivell BJ. Nephrotoxicity of ciclosporin A: short-term gain, long-term pain? Nephrol Dial Transplant. 2006; 21:2060–2063. [PubMed: 16728428]

19. Ponticelli C, Cucchiari D, Graziani G. Hypertension in kidney transplant recipients. Transpl Int. 2011; 24:523–533. [PubMed: 21382101]

20. Webster AC, Lee VW, Chapman JR, Craig JC. Target of rapamycin inhibitors (TOR-I; sirolimus and everolimus) for primary immunosuppression in kidney transplant recipients. Cochrane Database Syst Rev. 2006:CD004290. [PubMed: 16625599]

21. Brandriss MW. Methotrexate: suppression of experimental allergic encephalomyelitis. Science. 1963; 140:186–187. [PubMed: 14014958]

22. Corley CC Jr. Lessner HE, Larsen WE. Azathioprine therapy of "autoimmune" diseases. Am J Med. 1966; 41:404–412. [PubMed: 5330635]

23. Eiter LC, Hall NW, Day CS, Saluta G, Kucera GL, Bierbach U. Gold(I) analogues of a platinum-acridine antitumor agent are only moderately cytotoxic but show potent activity against Mycobacterium tuberculosis. J Med Chem. 2009; 52:6519–6522. [PubMed: 19803526]

24. Ahmed R, Salmi A, Butler LD, Chiller JM, Oldstone MB. Selection of genetic variants of lymphocytic choriomeningitis virus in spleens of persistently infected mice. Role in suppression of cytotoxic T lymphocyte response and viral persistence. J Exp Med. 1984; 160:521–540. [PubMed: 6332167]

25. Blattman JN, Antia R, Sourdive DJ, Wang X, Kaech SM, Murali-Krishna K, Altman JD, Ahmed R. Estimating the precursor frequency of naive antigen-specific CD8 T cells. J Exp Med. 2002; 195:657–664. [PubMed: 11877489]

26. Martins ET, Baruah H, Kramarczyk J, Saluta G, Day CS, Kucera GL, Bierbach U. Design, synthesis, and biological activity of a novel non-cisplatin-type platinum-acridine pharmacophore. J Med Chem. 2001; 44:4492–4496. [PubMed: 11728195]

27. Jia W, Pua HH, Li QJ, He YW. Autophagy regulates endoplasmic reticulum homeostasis and calcium mobilization in T lymphocytes. J Immunol. 2011; 186:1564–1574. [PubMed: 21191072]

28. Angelucci F, Sayed AA, Williams DL, Boumis G, Brunori M, Dimastrogiovanni D, Miele AE, Pauly F, Bellelli A. Inhibition of Schistosoma mansoni thioredoxin-glutathione reductase by auranofin: structural and kinetic aspects. J Biol Chem. 2009; 284:28977–28985. [PubMed: 19710012]

29. Sena LA, Li S, Jairaman A, Prakriya M, Ezponda T, Hildeman DA, Wang CR, Schumacker PT, Licht JD, Perlman H, Bryce PJ, Chandel NS. Mitochondria are required for antigen-specific T cell activation through reactive oxygen species signaling. Immunity. 2013; 38:225–236. [PubMed: 23415911]

30. Devadas S, Zaritskaya L, Rhee SG, Oberley L, Williams MS. Discrete generation of superoxide and hydrogen peroxide by T cell receptor stimulation: selective regulation of mitogen-activated protein kinase activation and fas ligand expression. J Exp Med. 2002; 195:59–70. [PubMed: 11781366]

31. Michalek RD, Nelson KJ, Holbrook BC, Yi JS, Stridiron D, Daniel LW, Fetrow JS, King SB, Poole LB, Grayson JM. The requirement of reversible cysteine sulfenic acid formation for T cell activation and function. J Immunol. 2007; 179:6456–6467. [PubMed: 17982034]

32. Laniewski NG, Grayson JM. Antioxidant treatment reduces expansion and contraction of antigen-specific CD8+ T cells during primary but not secondary viral infection. J Virol. 2004; 78:11246–11257. [PubMed: 15452243]

33. Crump KE, Langston PK, Rajkarnikar S, Grayson JM. Antioxidant treatment regulates the humoral immune response during acute viral infection. J Virol. 2013; 87:2577–2586. [PubMed: 23255789]

34. Crump KE, Juneau DG, Poole LB, Haas KM, Grayson JM. The reversible formation of cysteine sulfenic acid promotes B-cell activation and proliferation. Eur J Immunol. 2012; 42:2152–2164. [PubMed: 22674013]

35. Yang J, Gupta V, Carroll KS, Liebler DC. Site-specific mapping and quantification of protein S-sulphenylation in cells. Nat Commun. 2014; 5:4776. [PubMed: 25175731]

36. Luanpitpong S, Chanvorachote P, Nimmannit U, Leonard SS, Stehlik C, Wang L, Rojanasakul Y. Mitochondrial superoxide mediates doxorubicin-induced keratinocyte apoptosis through oxidative modification of ERK and Bcl-2 ubiquitination. Biochem Pharmacol. 2012; 83:1643–1654. [PubMed: 22469513]

37. D'Souza WN, Chang CF, Fischer AM, Li M, Hedrick SM. The Erk2 MAPK regulates CD8 T cell proliferation and survival. J Immunol. 2008; 181:7617–7629. [PubMed: 19017950]

38. Gorelik GJ, Yarlagadda S, Patel DR, Richardson BC. Protein kinase Cdelta oxidation contributes to ERK inactivation in lupus T cells. Arthritis Rheum. 2012; 64:2964–2974. [PubMed: 22549474]

39. Shaw JP, Utz PJ, Durand DB, Toole JJ, Emmel EA, Crabtree GR. Identification of a putative regulator of early T cell activation genes. Science. 1988; 241:202–205. [PubMed: 3260404]

40. Wu Z, Turner DR, Oliveira DB. IL-4 gene expression up-regulated by mercury in rat mast cells: a role of oxidant stress in IL-4 transcription. Int Immunol. 2001; 13:297–304. [PubMed: 11222498]

41. Angelini G, Gardella S, Ardy M, Ciriolo MR, Filomeni G, Di Trapani G, Clarke F, Sitia R, Rubartelli A. Antigen-presenting dendritic cells provide the reducing extracellular microenvironment required for T lymphocyte activation. Proc Natl Acad Sci U S A. 2002; 99:1491–1496. [PubMed: 11792859]
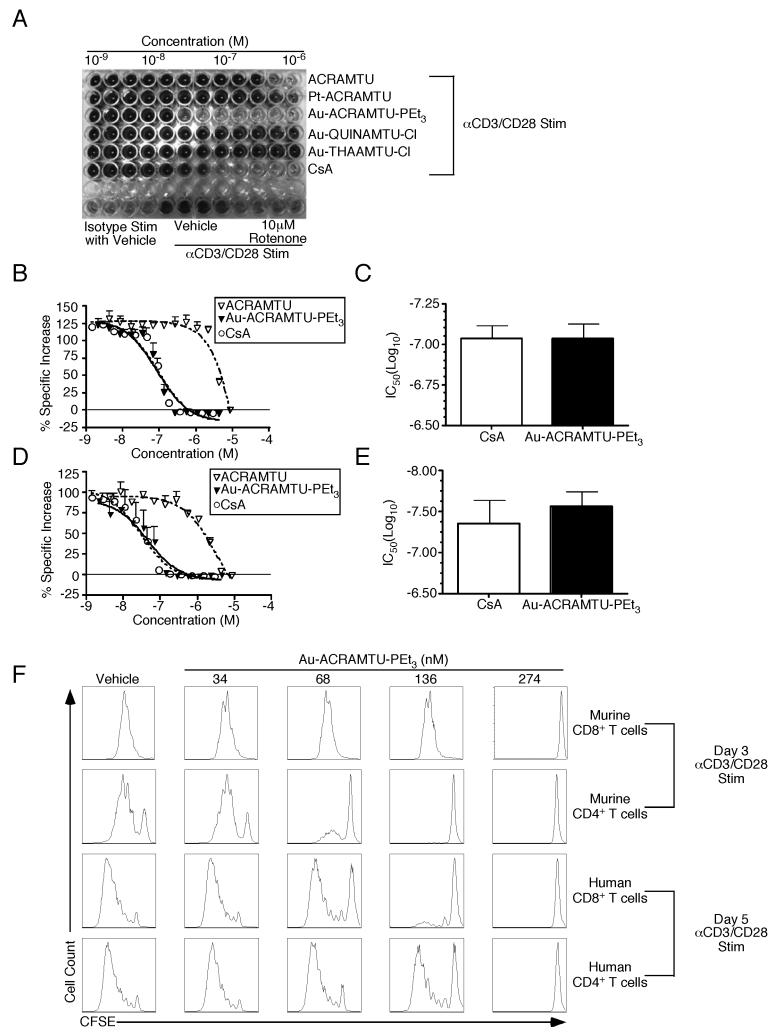
Figure 1. Incubation with Au-ACRAMTU-PEt$_3$ inhibits naïve murine and human T cell proliferation

Splenocytes were isolated from naïve C57BL/6 mice, and CD8$^+$ T cells (A-C) or CD4$^+$ T cells (D and E) were purified by magnetic microbeads. Naïve CD8$^+$ T cells or CD4$^+$ T cells were treated with drugs over a range of concentrations (serial 2-fold dilutions from right-to-left, starting with 10^{-6} to 10^{-9}M) for 60 min at 37°C, stimulated with plate-bound CD3 and CD28 Abs, and incubated for 72 h. Celltiter 96 Aqueous One Solution from Promega was added to each well, absorbances were read at 490 nm, and percent specific increases were calculated. Dose-response curves were generated for each drug (B and D), and the average IC$_{50}$ was determined (C and E). Naïve CD8$^+$ T cells or CD4$^+$ T cells from naïve C57BL/6 mice or healthy human donors were purified, treated with drug for 60 min at 37°C, and activated with αCD3 and αCD28 Abs. Proliferation of murine and human CD8$^+$ T cells and CD4$^+$ T cells (F) was assessed by loss of CFSE fluorescence after activation. Histograms are gated on 7AAD$^-$ cells. Representative plots are shown for 4 independent experiments. MTS assay results are from 3-6 independent experiments. The mean and standard deviation are plotted. *, significant difference between vehicle- and Au-ACRAMTU-PEt$_3$-treated cells , p 0.05.
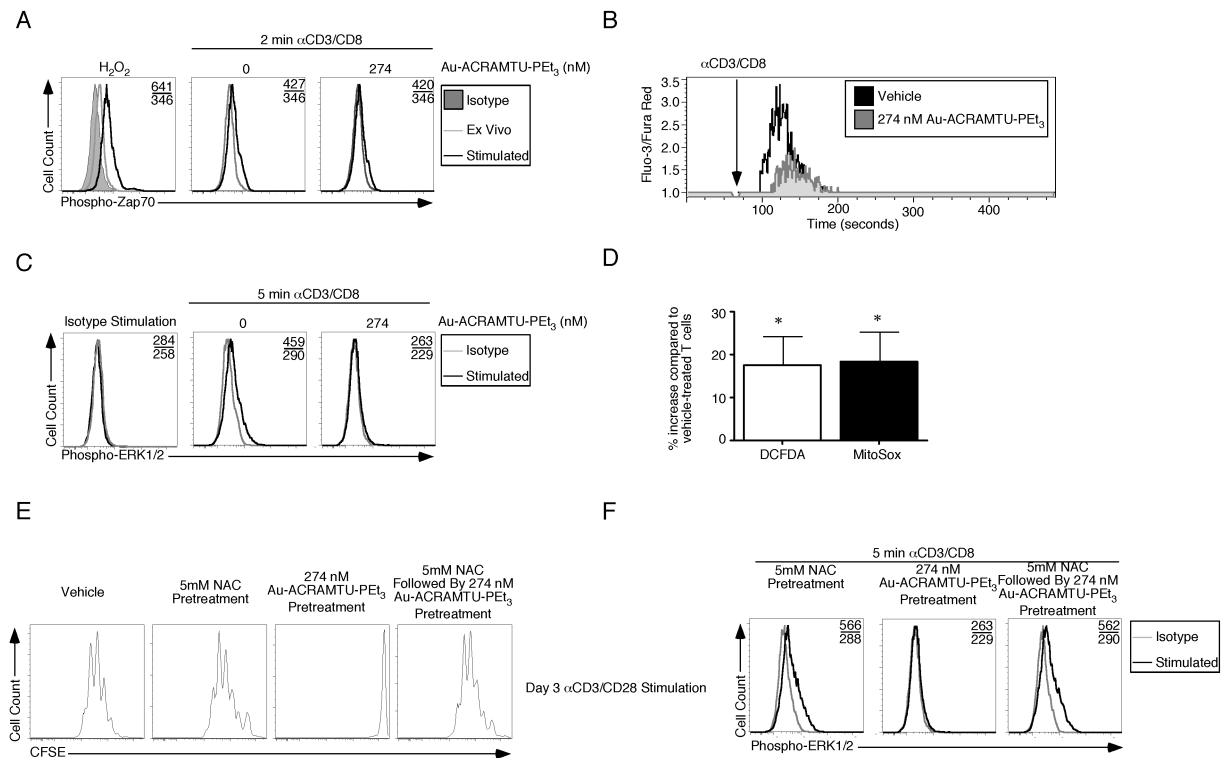
Figure 2. Au-ACRAMTU-PEt$_3$ incubation inhibits calcium flux and ERK1/2 phosphorylation during CD8$^+$ T Cell activation

(A) Magnetic microbead purified CD8$^+$ T cells were incubated with 0.1% DMF control or Au-ACRAMTU-PEt$_3$ for 30 min. After washing, cells were incubated with biotin-labeled anti-CD3 and anti-CD8 antibodies or isotype control. Cross-linking was induced by incubation with streptavidin for 2 minutes followed by intracellular staining with isotype or anti-phospho-ZAP70 antibodies. Numbers in the upper right hand corners indicate the stimulated and unstimulated m.f.i. The H$_2$O$_2$ plot is included as a positive control. (B) Purified CD8$^+$ T cells were incubated with Fura-Red-AM and Fluo-3-AM in the presence of Au-ACRAMTU-PEt$_3$ for 30 min. After washing, cells were resuspended in PBS supplemented with FCS, incubated with biotin-labeled anti-CD3 and anti-CD8 antibodies and were acquired on a cytometer for 1 min prior to incubation with streptavidin to induce crosslinking. Acquisition was resumed for an additional 5 min and 30 s. The ratio of Fluo-3 to Fura-Red fluorescence was recorded as a function of time. (C) For MAPK measurement cells were harvested after 5 minutes of stimulation and stained with anti-phospho-ERK1/2 antibodies. (D) Naïve CD8$^+$ T cells were treated with Au-ACRAMTU-PEt$_3$ and labeled with either DCFDA or MitoSox for 30 minutes and acquired. The increase in m.f.i. compared to 0.1% DMF control-treated samples is plotted. Three mice were examined in three independent experiments. (E) Naïve CD8$^+$ T cells were treated with media or 5 mM NAC for 1 h followed by treatment with media or 274 nM Au-ACRAMTU-PEt$_3$ for 1 h at 37°C. Cells were then activated with CD3 and CD28 Abs. Proliferation was assessed by loss of CFSE fluorescence after activation. Representative plots are shown for 3 mice in 2 independent experiments. (F) CD8$^+$ T cells were pretreated with NAC, Au-ACRAMTU-
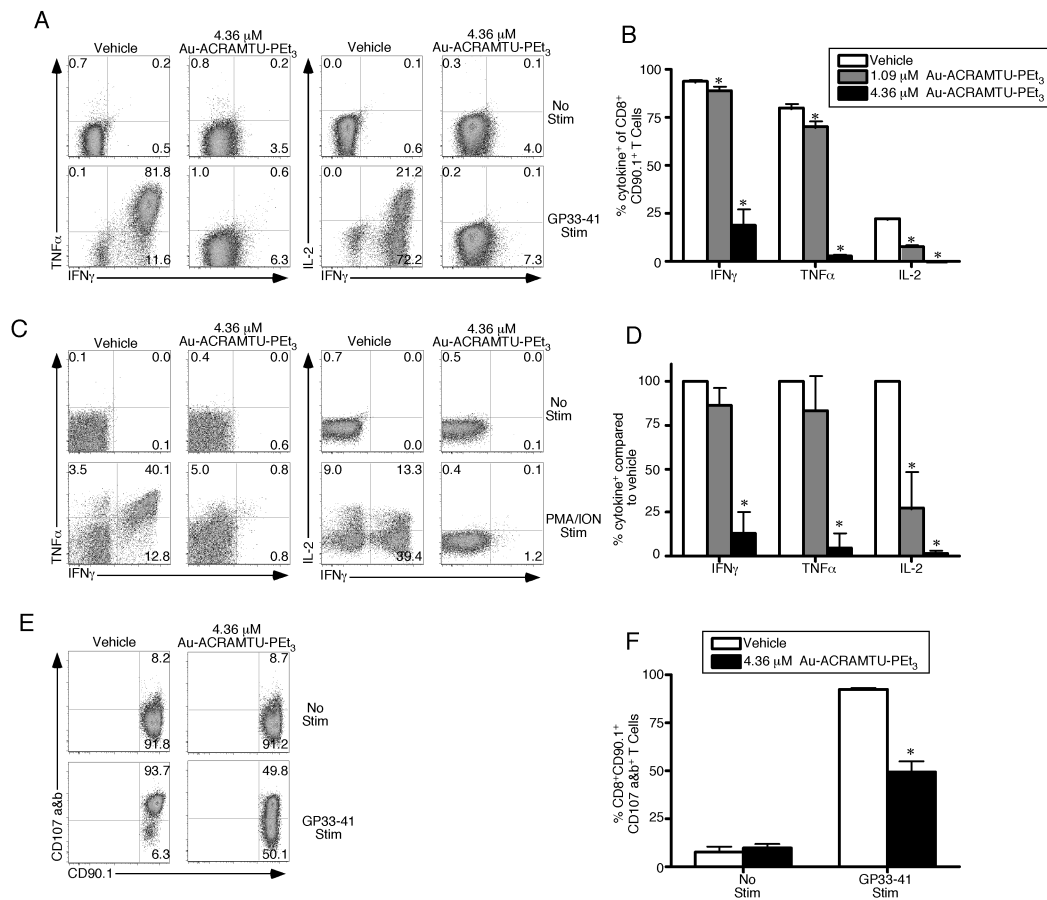
PEt$_3$, or NAC and Au-ACRAMTU-PEt$_3$ and ERK1/2 staining was performed as described above. Four mice were examined in three independent experiments.

Figure 3. Incubation with Au-ACRAMTU-PEt$_3$ inhibits murine and human effector T cell function

C57BL/6 mice were injected intravenously with 10^5 Thy1.1$^+$ (CD90.1$^+$) P14 cells and were subsequently infected with 2×10^5 pfu of LCMV Armstrong. On day 8 postinfection, mice were sacrificed, the spleen was removed, splenocytes were treated with vehicle or Au-ACRAMTU-PEt$_3$ for 1 h at 37°C, and stimulated (A) with GP33-41 peptide and labeled (E and F) with anti-CD107a/b Abs for 5 hours at 37°C. Following stimulation, cells were stained with anti-CD8, anti-CD90.1, IFNγ, TNFα, and IL-2 Abs. Dot plots (A) are gated on CD90.1$^+$ CD8$^+$ T cells, and the number in the plots indicates the percentage of CD90.1$^+$ CD8$^+$ T cells that are present in that quadrant. The percentage of CD8$^+$ CD90.1$^+$ T cells that produced IFN-γ, TNF-α, and IL-2 (B) or CD107a and b (F) was determined. The mean and standard deviation are plotted. Five to six mice were analyzed in a minimum of 2 independent experiments. PBMCs were isolated from healthy human donors and were then treated with vehicle or Au-ACRAMTU-PEt$_3$ for 1 h at 37°C followed by stimulation (C) with PMA/ION for 5 hours at 37°C. Following stimulation, cells were stained with CD8, IFNγ, TNFα, and IL-2 Abs. Dot plots (C) are gated on CD8$^+$ T cells, and the number in the plots indicates the percentage of CD8$^+$ T cells that are present in that quadrant. (D) The percentage of drug-treated CD8$^+$ T cells that produced IFN-γ, TNF-α, and IL-2 compared to vehicle-treated CD8$^+$ T cells was determined. The mean percent of vehicle cytokine production and standard deviation are plotted. Four subjects were analyzed in four
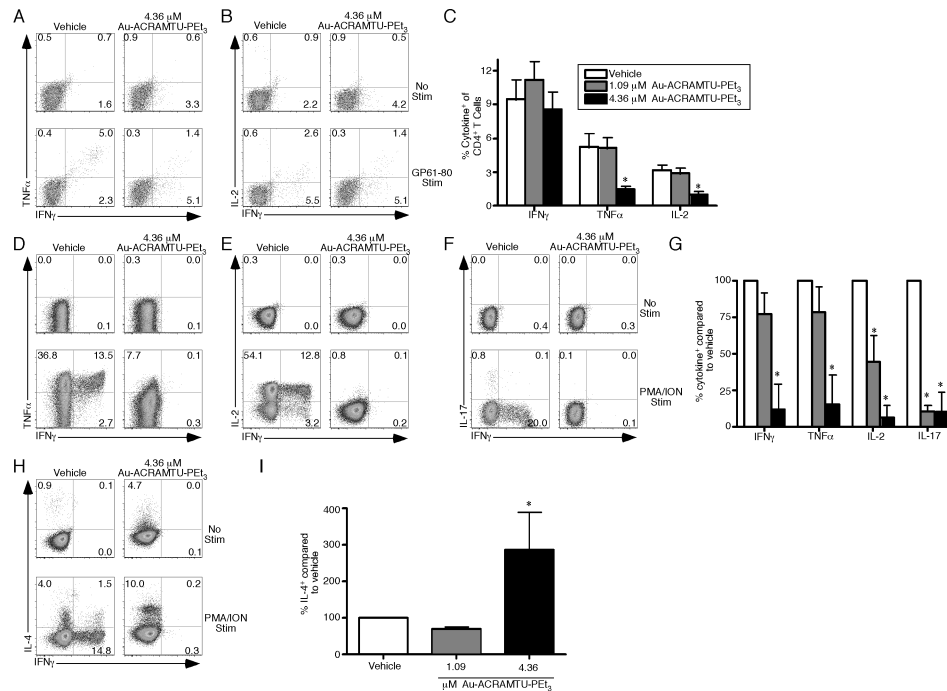
independent experiments. *, significant difference between vehicle and Au-ACRAMTU-PEt$_3$ treated cells, p 0.05.

**Figure 4. Incubation with Au-ACRAMTU-PEt$_3$ inhibits cytokine production of murine and human CD4$^+$ T cells**

C57BL/6 mice were infected with 2×10^5 pfu of LCMV Armstrong. On day 8 postinfection, mice were sacrificed, the spleen was removed, splenocytes were treated with vehicle or Au-ACRAMTU-PEt$_3$ for 1 h at 37°C, and stimulated (A-C) with GP61-80 peptide for 5 hours at 37°C. Following stimulation, cells were stained with CD4, IFNγ, TNFα, and IL-2 Abs. Dot plots (A and B) are gated on CD4$^+$ T cells, and the number in the plots indicates the percentage of CD4$^+$ T cells that are present in that quadrant. (C) The percentage of CD4$^+$ T cells that produced IFNγ, TNFα, and IL-2 was determined. The mean and standard deviation are plotted. Six mice were analyzed in two independent experiments. (D-I) PBMCs were isolated from healthy human donors and were then treated with vehicle or Au-ACRAMTU-PEt$_3$ for 1 h at 37°C followed by stimulation with PMA/ION for 5 hours at 37°C. Following stimulation, cells were stained with CD4, IFNγ, TNFα, IL-2, IL-17, and IL-4 Abs. Dot plots (D-F, and H) are gated on CD4$^+$ T cells, and the number in the plots indicates the percentage of CD4$^+$ T cells that are present in that quadrant. (G) The percentage of drug-treated CD4$^+$ T cells that produced IFNγ, TNFα, IL-2, and IL-17 (G) or IL-4 (I) compared to vehicle-treated CD4$^+$ T cells was determined. The mean percent of vehicle cytokine production and standard deviation are plotted. Four subjects were analyzed in four independent experiments. *, significant difference between vehicle and Au-ACRAMTU-PEt$_3$ treated cells, p 0.05.
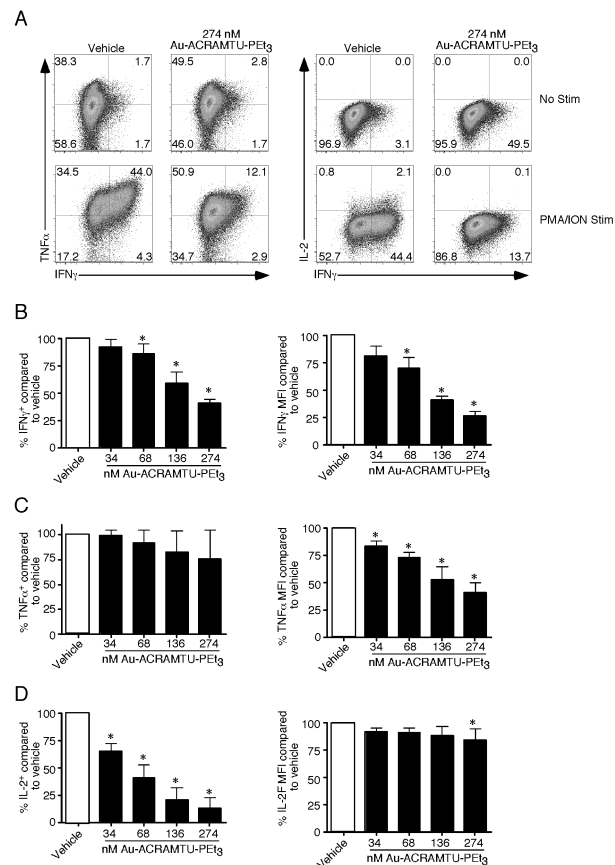
Figure 5. Au-ACRAMTU-PEt$_3$ treatment inhibits CD8$^+$ T cell cytokine production in an autonomous manner

Splenocytes were isolated from naïve C57BL/6 mice, and CD8$^+$ T cells were purified by magnetic microbeads. Naïve CD8$^+$ T cells stimulated with plate-bound CD3 and CD28 Abs in the presence of 2U/ml recombinant murine IL-12 for 2 days. Cells were removed from Ab coated plates and allowed to rest overnight and were then pretreated for 1 hour at 37°C with the indicated concentration of Au-ACRAMTU-PEt$_3$ followed by PMA and ION stimulation for 5 hours. Afterwards cells were intracellularly stained for their production of IFNγ, TNFα and IL-2 (A). The number in the plots indicates the percentage of CD8$^+$ T cells that are present in that quadrant. For IFNγ (B), TNFα (C), and IL-2 (D) the percentage of cells positive for each cytokine relative to vehicle treated samples was determined. Additionally, the MFI of each cytokine was compared to vehicle treated samples. The mean percent of vehicle cytokine production and standard deviation are plotted. Four lines were analyzed in three independent experiments. *, significant difference between vehicle and Au-ACRAMTU-PEt$_3$ treated cells, p 0.05.
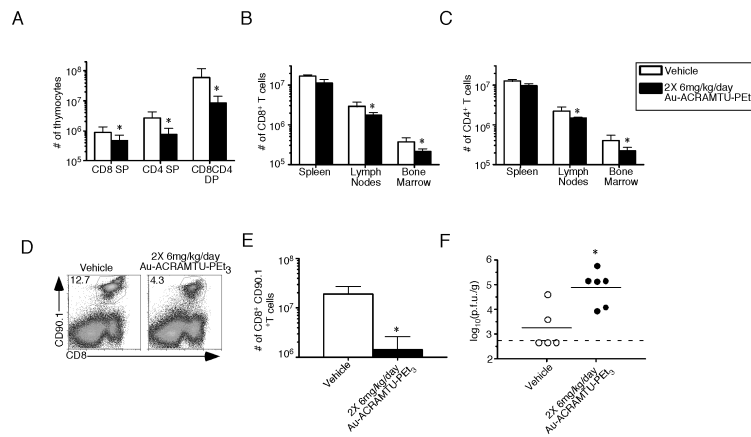
Figure 6. Treatment with Au-ACRAMTU-PEt₃ reduces expansion of virus-specific CD8⁺ T cells following acute LCMV infection

Naïve C57BL/6 mice were treated with either vehicle or 6 mg/kg of Au-ACRAMTU-PEt$_3$ every 12 hours for 8 days. Mice were sacrificed on day 8, and the spleen, lymph nodes, bone marrow, and thymus were removed. Cells were stained with CD8 and CD4 Abs, and the numbers of CD8 SP, CD8CD4 DP, and CD4 SP T cells in the thymus were quantified (A). The total numbers of CD8⁺ (B) and CD4⁺ (C) T cells were also quantified in the spleen, lymph nodes, and bone marrow. Means and standard deviations are shown for 3 mice in each group. (D and E) Naïve C57BL/6 mice were treated with either vehicle or 6 mg/kg of Au-ACRAMTU-PEt$_3$. After 4 hours, mice were injected intravenously with 10^5 Thy1.1⁺ (CD90.1⁺) P14 cells and were subsequently infected with 2×10^5 pfu of LCMV Armstrong. A maintenance dose of vehicle or Au-ACRAMTU-PEt$_3$ was administered every 12 hours for 8 days. On day 8 postinfection, mice were sacrificed, the spleen was removed, and cells were stained with CD8 and CD90.1 Abs (D) and D^{b}GP33-41 tetramer. The numbers of CD8⁺ CD90.1⁺ T cells were quantitated (E), and the mean and standard deviation are shown. (F) The viral load in the spleen at day 8 was quantitated by plaque assay. Five to six mice were examined in 2 independent experiments. *, significant difference between vehicle- and Au-ACRAMTU-PEt$_3$-treated mice, $p \; 0.05$.